

## Thermal Expansions of Solid Argon, Krypton, and Xenon above 1 K\*

C. R. Tilford<sup>†</sup> and C. A. Swenson

*Institute for Atomic Research and Department of Physics, Iowa State University, Ames, Iowa 50010*

(Received 6 August 1971)

A differential parallel-plate capacitance dilatometer has been used to measure the linear thermal-expansion coefficients of free-standing samples of solid argon (1–35 K), krypton (1–45 K), and xenon (1–105 K). The present data for argon and krypton are systematically larger than existing x-ray lattice-parameter data above 20 K by a constant proportionality factor which varies from 1 to 3% for different runs and different samples and which most likely is due to bonding of the samples to the capacitor plates. These data have been normalized using the x-ray results. The xenon results agree with other published data without the use of a scale factor. Temperature-dependent Grüneisen parameters  $\gamma$  are calculated for these solids using available thermodynamic data. These calculations give  $\gamma_0 = 2.7 \pm 0.1$  for argon,  $2.67 \pm 0.07$  for krypton, and  $2.5 \pm 0.1$  for xenon, with the major uncertainty occurring through the bulk-modulus data.

### INTRODUCTION

The rare-gas solids (RGS) neon, argon, krypton, and xenon long have been used as model substances for lattice dynamical calculations of thermodynamic properties since their closed electronic shells result in very similar interatomic potential functions for the solid and for the dilute gas states. The work with gases suggested that the combination of a relatively long-range van der Waals attractive interaction and a strong repulsive interaction due to the closed shells could be approximated by simple analytical expressions on which most of the theoretical calculations for the solid have been based. However, the same weak forces which make the RGS attractive for theoretical calculations also give rise to physical properties which make them difficult to work with experimentally. For instance, the RGS are characterized by low triple-point temperatures (which vary from 165 K for xenon to 24 K for neon) high vapor pressures at the triple points (usually greater than 0.5 atm), low yield strengths, low thermal conductivities, high heat capacities and thermal expansions, and the ability to bond firmly to any substance. Because of the difficulties involved in working with these solids, there have been very few good quality experimental data available for the RGS until recent years.

The availability of precision data led to the conclusion that conventional theoretical approaches, such as those described by Horton,<sup>1</sup> were not adequate to explain quantitatively the experimental results. In particular, the relatively large anharmonicity in these solids (large atomic-vibration amplitudes), especially at high temperatures, makes the application of perturbation theory questionable, and the most important recent calculations of high-temperature thermodynamic properties have involved the self-consistent phonon approach which

was developed for solid helium.<sup>2</sup> The application of the theory is relatively more simple for the heavier RGS (argon, krypton, and xenon), for which Klein *et al.*<sup>3</sup> have summarized results of normal perturbation theory and improved self-consistent phonon calculations. Anharmonic effects are small at low temperature for these solids and the results of all of the calculations appear to converge to the same answers in this limit. In any case, none of the theories are completely successful in explaining all facets of the existing experimental data.

This failure probably is due to a great extent to the over simplified nature of the Mie-Lennard-Jones potentials which are used in strictly two-body calculations rather than to inadequacies in the theories themselves.<sup>3</sup> Recently, Barker and his colleagues have used realistic two-body interactions, which are based on gas data as well as  $T=0$ ,  $P=0$  solid properties and three-body interactions of the Axilrod-Teller type, to calculate anharmonic thermodynamic properties of solid argon<sup>4,5</sup> and solid krypton.<sup>6</sup> This work has been quite successful in predicting the form of the temperature dependence of the low-temperature specific heat and also of the thermal expansion, as we will discuss below. Jelinek<sup>7</sup> has used a Morse potential in a two-body quasiharmonic calculation for these solids. The experimental zero-pressure cohesive energy and lattice parameter are used in all calculations to assist in establishing the potential parameters, while in addition, Barker *et al.* make use of the experimental  $T=0$  value of the Debye temperature, and Jelinek utilizes the  $T=0$ ,  $P=0$  values of the bulk modulus.

The prediction of the temperature dependence of the volume thermal-expansion coefficient

$$\beta = V^{-1} \left( \frac{\partial V}{\partial T} \right)_P = B_T^{-1} \frac{\partial^2 F}{\partial T \partial V} \quad (1)$$

is a severe test for the theory since  $\beta$  involves a mixed second derivative of the Helmholtz free energy  $F$ . In effect, these calculations are sensitive to the third derivatives of the potential function, while both the constant-volume specific-heat and the  $T=0$  bulk-modulus  $B_T$  calculations involve only the second derivatives. Much of the recent theoretical work has been compared with the precision x-ray lattice-constant measurements of Simmons and his co-workers,<sup>8-11</sup> who studied the effects of both temperature and pressure on single crystals of neon, argon, and krypton. While undoubtedly the x-ray technique offers the most direct method for obtaining thermal-expansion data for hard to handle substances like the RGS, it lacks sufficient sensitivity to obtain accurate data for temperatures below 15 or 20 K except for neon, even at the precision attained by Simmons and his co-workers. Optical interferometer measurements which have been reported for krypton<sup>12,13</sup> have greater reported resolution than the x-ray measurements ( $10^{-6}$  in  $\Delta L/L_0$ ), but this is far from the resolution of  $10^{-10}$  which is required to obtain meaningful data at temperatures where the continuum or Debye model is valid (0.01 to 0.03  $\Theta_D$ , or from 1 to 5 K).

We have given a preliminary report<sup>14</sup> of the use of a three-terminal capacitance dilatometer to measure with this type of resolution the thermal-expansion coefficient of free-standing solid-argon samples at temperatures down to 1 K. The present paper gives the details of these earlier measurements, and reports similar data which we have obtained for krypton and xenon. The xenon measurements extend to 105 K since precise x-ray measurements do not exist for this solid. A similar

capacitance technique, but with samples confined by bellows, has been used to measure the thermal expansion of solid methane<sup>15</sup> and the thermal expansion and compressibility of solid nitrogen.<sup>16</sup>

#### EXPERIMENTAL

The three-terminal capacitance technique for measuring thermal expansions developed by White<sup>17,18</sup> used the highly stable and precise three-terminal ratio-transformer bridge developed by Thompson.<sup>19</sup> The three-terminal design, where the third terminal is a grounded guard around one or both leads of the capacitor, eliminates the effect of "stray" capacitances by defining a unique geometrical capacitance and hence allows the full use of the high resolution of a ratio-transformer bridge.

The "normal" configuration of the differential cell, as used by White,<sup>17,18</sup> is sketched in Fig. 1. A guarded upper plate is mounted above a second plate which is attached to the sample; the separation between these plates depends on the difference in the expansions of the cell body and of the sample. This gap length  $L_g$  is related to the plate area and the capacitance  $C$  by

$$L_g = \epsilon_0 A / C, \quad (2)$$

and the length sensitivity is given by

$$\frac{dC}{dL_g} = \frac{-\epsilon_0 A}{L_g^2}. \quad (3)$$

The thermal expansions for the RGS are so large (3% between the triple point and 0 K for argon, for instance) when compared with copper (effectively zero for this interval) that even for zero initial

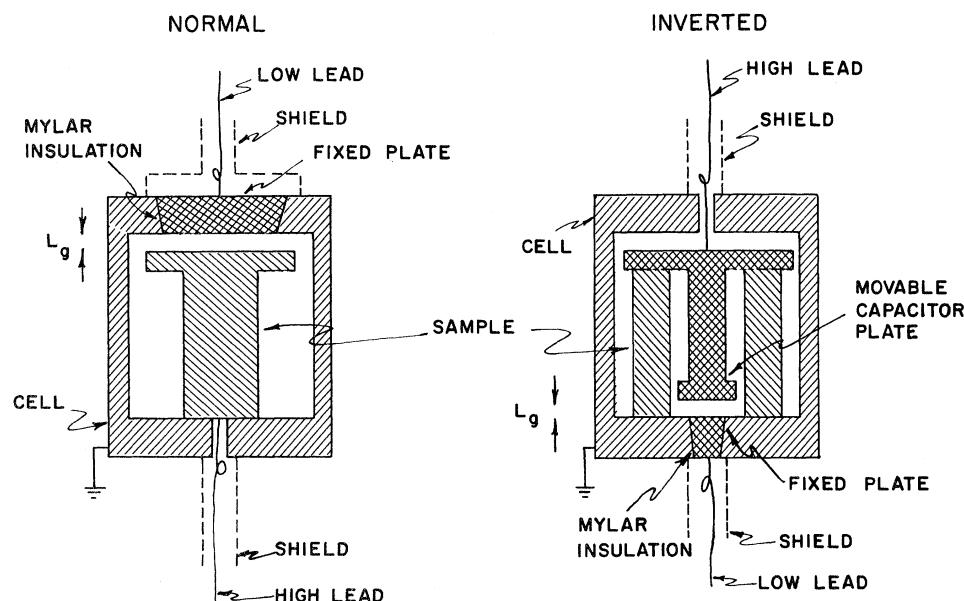


FIG. 1. Normal and inverted capacitance cells. For the inverted cell, the capacitor gap decreases with decreasing temperature giving maximum length sensitivity at low temperatures.

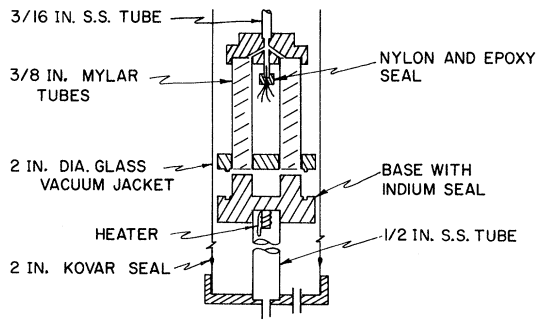


FIG. 2. Sketch of the sample-growing apparatus.

gap at high temperature the sensitivity is greatly reduced at low temperatures where it is most needed. Therefore, we have used an "inverted" configuration for our measurements on the RGS (also shown in Fig. 1) for which the gap closes with decreasing temperature.

The use of an inverted cell suggests a sample geometry in the form of a hollow cylinder with the top capacitor plate hanging down through the hole in the center of the sample. However, since the RGS readily bond to other substances, large strains are liable to be caused by differential contraction between the capacitance cell and the sample. These strains can be minimized by replacing the hollow cylinder with three posts which are placed symmetrically about the periphery of the cylinder. The differential contraction now takes place across the smaller diameter of the individual posts. While this configuration lessens the differential contraction problem, the posts may well tip over during the assembly of the capacitance cell since this operation must be carried out under rather awkward conditions. In order to allow both kinds of samples to be used if necessary, and to simplify the design to the capacitance cell, the samples originally were grown in one Dewar and then for the actual expansion measurements were transferred to a second Dewar which contained the capacitance cell. When it was determined that the three-post configuration would work, the capacitance cell was modified to include the sample-growing apparatus.

#### Sample Preparation

The sample-growing apparatus is sketched in Fig. 2. The samples are grown inside  $\frac{3}{8}$ -in.-diam tubes which are epoxied together from 0.0015-in. Mylar. The three tubes are equally spaced on a  $\frac{7}{8}$ -in.-diam circle and are epoxied into top and bottom endpieces. A  $\frac{3}{16}$ -in.-diam stainless-steel tube is soldered into the top brass endpiece to connect the mold to an outside gas-handling system. Wires for heaters and thermocouples also come down this tube and exit through a nylon and epoxy

seal. A heater wound on the top endpiece is used to control the rate of sample growth. The bottom endpiece, made from copper or brass, has a heater and thermocouple attached to it so that it can be maintained slightly above the freezing point when the samples are dropped from the tubes. There are sockets for twelve 2-56 socket-head screws on the periphery of the bottom endpiece and a raised ridge on its bottom. This ridge fits into an indium-filled groove in the base and the twelve screws are used to clamp the two pieces together to seal the bottoms of the tubes. The base has three pedestals which fit inside the Mylar tubes past the bottom endpiece so that the samples grow entirely within the Mylar tubes. The base is mounted on a 6-in.-long 0.5-in.-diam stainless-steel tube and has a heater so that its temperature can be controlled. The sample-growing apparatus is mounted in the bottom of a 4.5-ft-long glass vacuum jacket, which is contained within a set of glass Dewars. All assembly and disassembly in both the sample apparatus and capacitance cell is done with Allen wrenches soldered into the ends of 4.5-ft-long  $\frac{1}{8}$ -in.-diam stainless-steel rods which pass through rotating vacuum seals in the Dewar head.

Although they were never used, hollow cylinder samples were grown using basically the same apparatus. A single 1.25-in.-diam Mylar mold was used and the base had a 0.5-in.-diam closed tube made of 0.00025-in. Mylar mounted in the center. This tube was inflated with He gas during sample growth and then collapsed when the sample was removed, leaving a 0.5-in. hole in the center.

The sample-growth procedure is as follows. The indium seal is sprayed with a Teflon dispersion to prevent cold soldering, the tube assembly is screwed to the base, the vacuum chamber and mold are thoroughly pumped out, gas is let into the mold, and liquid nitrogen is transferred into the Dewar. The tubes gradually fill with liquid to a height such that the solid samples will be  $30 \pm 1$  mm long. The mold then is sealed off from the gas supply and the base is allowed to cool so that the samples grow from the bottom. The heater on the top endpiece is used to keep the pressure above the triple point until the sample is finished. This produces optically clear, void-free, but undoubtedly polycrystalline samples in 4 or 5 h.

Once solidification is completed the samples are cooled to about 20 K below their triple point and the screws holding the mold to the base are unscrewed. The base is heated rapidly to melt the thin layer of solid gas bonding it to the bottom endpiece and the mold is pulled free with the samples bonded to the inside of the mylar tubes. The vacuum chamber is immediately filled with He gas to reduce sublimation of the samples. In the original apparatus the mold and samples then were maneu-

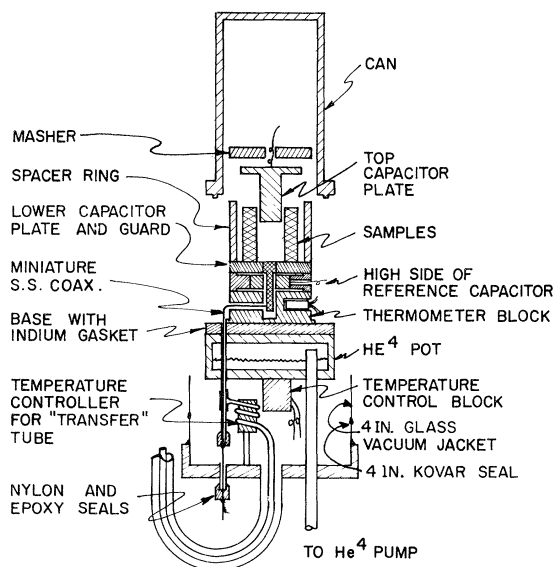


FIG. 3. Sketch of the capacitance cell.

vered into a small transfer Dewar and transferred to the Dewar containing the capacitance cell.

It might be noted that, in spite of their reputation for "fragility," none of the 50 or more samples grown in the course of this experiment ever were observed to break or shatter. This was in spite of their being subjected, intentionally and unintentionally, to a wide range of mechanical and thermal shock at temperatures well below their triple points. Samples were observed to bend under their own weight and sublimation was a constant problem.

#### Capacitance Cell

The copper capacitance cell is sketched in Fig. 3. The bottom capacitor plate has a  $2^\circ$  taper and is wrapped with two turns of 0.001-in. Mylar before being pressed into a mating hole in the center of the guard ring. The two pieces then are machined and lapped flat together. The guard ring also serves as the base on which the samples rest during the measurement and, in the second version of the capacitance cell, contains the base of the sample-growing apparatus. The bottom capacitor plate extends downward to form one side of a reference capacitor which is used to measure the dielectric constant of the gas in the sample chamber. Although not used, this would allow compressibility measurements to be made by compressing the sample with gaseous helium. When not in use the high side of the reference capacitor is grounded. Directly underneath the reference capacitor is a thermometry block which contains holes for germanium and platinum resistance thermometers and thermal anchors for their leads. The upper capacitor plate consists of a flat disc which rests on the

samples and a cylindrical rod (1.2 cm diam and 2.9 cm long) which establishes the reference length of copper for the cell. The role of the masher plate and the spacer ring will be detailed in a later description of sample loading and cell assembly.

The capacitance cell is isolated from the vacuum jacket surrounding it by a large can which screws down onto an indium gasket on the base plate. All leads, including miniature stainless-steel coaxial cables for the capacitor leads, enter the cell through nylon and epoxy seals. Helium exchange-gas pressure inside the cell is regulated through a single vacuum-jacketed temperature-controlled "transfer tube" which goes up to the Dewar head. Temperature control of the tube eliminates "cold spots" which cause rapid sublimation when the temperature of the samples is raised above about 40 K. A  $\text{He}^4$  pot into which helium is condensed cools the apparatus as low as 1 K. Above 2 K a temperature-control block with heaters and resistance-thermometer sensors is used in conjunction with an electronic temperature controller to regulate the temperature of the cell. The entire cell is supported by three 0.25-in.-diam stainless-steel tubes which are soldered into the brass base of a 4.5-ft-long 4-in.-diam glass vacuum jacket. One of the three tubes acts as a pumping line for the  $\text{He}^4$  pot. The entire apparatus rests inside a double set of glass Dewars with vertical viewing slits. During a measurement the liquid in the helium Dewar is pumped to a temperature below the  $\lambda$  point and the nitrogen Dewar is pumped down to the triple point and backfilled with helium gas to prevent boiling.

#### Sample Manipulation, Cell Assembly

Once a set of samples is grown, the samples are positioned above the capacitance cell, still attached to the inside of the Mylar tubes. The tube assembly then is lowered down inside the spacer ring so that its bottom end piece is 1 or 2 mm above the guard ring in the cell base. The vacuum space is pumped out and the heaters wound on the tubes turned on so that the surface of the samples sublimates away. After several minutes the samples slide down the tubes and rest on the guard ring, and the mold is carefully pulled away, leaving the samples free standing. By this time the ends of the samples are well rounded because of sublimation. This caused two sets of krypton and two sets of xenon samples to tip over when the mold was withdrawn at 77 K. However, argon samples dropped at temperatures as low as 55 K, krypton samples dropped at 95 K, and xenon samples dropped at 135 K all remained standing. This is most likely because above a certain temperature the sample rapidly bonds to the copper guard ring. A rather crude experiment indicated that the bonding temperature for xenon is

between 95 and 100 K.

The top capacitor plate and "masher" (Fig. 3) are stored in a bulge in the upper part of the vacuum jacket while the samples are dropped from the mold. The capacitor plate hangs from the masher which is supported by a stainless-steel tube which passes through a vacuum seal in the Dewar head. After the mold is removed, the masher and top capacitor plate are lowered until the capacitor plate rests on the tops of the samples. The masher then is screwed down to the spacer, "mashing" the samples to a uniform length which is determined by the spacer height. Upon cooling the samples shrink, leaving the 58-g capacitor plate supported only by the insulating samples. The low yield strengths<sup>20</sup> and high annealing rates of the RGS should minimize the strains introduced by this process. The can now is placed in the vacuum jacket, is allowed to cool, and then is lowered down onto the base plate and is screwed down onto the indium gasket. This effects a fairly reliable helium leak tight seal, even at 55 K.

During the 3 to 6 h necessary to complete the sample manipulation and to assemble the cell, a stream of helium gas is blown up from the bottom of the vacuum jacket via a tube which passes down through the inner Dewar from the Dewar head. If enough gas is used, this prevents air from entering the top of the vacuum jacket, which often is only loosely sealed. If excessive quantities are used, this procedure causes severe sublimation and the samples may become too short to use.

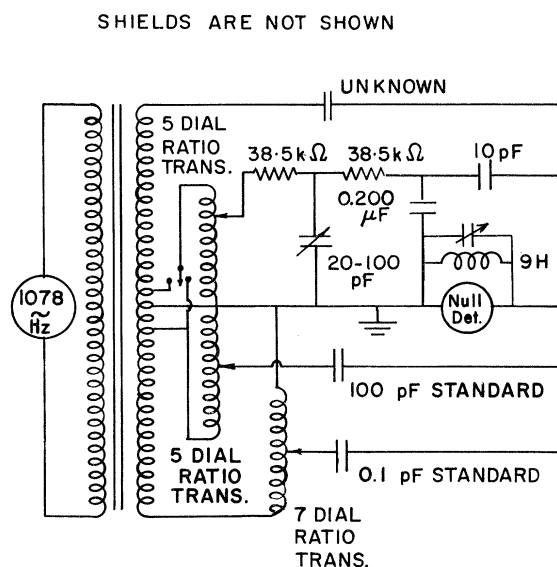
During assembly of the capacitance cell, the inner Dewar contains liquid nitrogen or a nitrogen-oxygen mixture. When the assembly of the cell is completed, the vacuum jacket is pumped out, the liquid is blown out of the inner Dewar, liquid helium is transferred into the inner Dewar, and the apparatus is allowed to cool to helium temperatures over a 5- to 10-h period. The helium exchange-gas pressure inside the capacitance cell is varied from one atmosphere at nitrogen temperatures to about  $10 \mu$  at helium temperatures.

#### Capacitance Bridge

The capacitance bridge shown in Fig. 4 is essentially identical to that described by White.<sup>17</sup> The main transformer is wound on a high-permeability Supermalloy toroid with a ratio accurate to 1 part in  $10^5$  or better. The seven-dial ratio transformer is a Gertsch model 1011R Ratiotran and the five-dial ratio transformer is a Gertsch model RT-60. The 100-pF standard capacitor is a General Radio model 1404B and the 0.1-pF standard capacitor is a General Radio model No. 1403N. The capacitance standards are temperature controlled to better than  $10^{-3}$  K, giving a stability of better than 1 part in  $10^8$  for the 100-pF standard over the course of a day. The

cable or shield capacitance shunting the detector is tuned out by a high-Q inductor wound on a ferrite core. A change in capacitance of  $10^{-7}$  pF can be detected using a sensitive lock-in detector and 100-V peak to peak across the capacitors. At this level of sensitivity, serious problems sometimes were encountered with noise and drifts when the bridge was connected to the capacitance cell in the Dewar at low temperatures. These appeared to be correlated with small motions of the inner Dewar which were caused by slight pressure changes in the Dewar. These effects later were traced to inadequate grounding of one of the coaxial cables.

Our thermometry is quite conventional, and involves an NBS-calibrated Leeds and Northrup (L and N) model 8164 platinum-resistance thermometer above 15 K and a locally calibrated commercial germanium-resistance thermometer ( $R_{4K} = 335 \Omega$ ) for temperatures between 1 and 28 K. The germanium thermometer calibration is essentially in terms of the constant-volume-gas-thermometer (CVGT) scale of Rogers *et al.*,<sup>21</sup> and is based on the NBS platinum scale above 18 K. The calibrations of the two thermometers were cross-checked *in situ* in the overlap region and agreed at all points to  $\pm 2$  mK. The germanium thermometer also was calibrated in terms of the liquid-helium vapor-pressure scale  $T_{58}$  below 4.2 K, and this scale was used in the analysis of the data in this region. There is a discrepancy between the CVGT scale and  $T_{58}$  which is of the order of 0.2% near 4 K, and, as was discussed for some heat capacity measurements,<sup>22</sup> this can result in ambiguities of 0.5% or so in data which have a  $T^3$  dependence. This offers no basic problem in the present mea-



surements, which, for various reasons to be discussed below, have an accuracy of  $\pm 1\%$  in this temperature region. While we have access to a much smoother temperature scale,<sup>23</sup> we have not chosen to correct our data to correspond to it.

The thermometer resistances are determined by comparison with L and N NBS-type standard resistances using a current-reversal potentiometric technique. The basic measuring instruments included an L and N type K-5 potentiometer and a Keithley model 150A microvoltmeter as a null detector which drives a chart recorder. Thermometer currents are selected to give a temperature sensitivity of 1 mK at all temperatures, and self-heating effects are determined to be less than this sensitivity.

#### EXPERIMENTAL RESULTS

Thermal-expansion data are obtained by taking simultaneous temperature and capacitance readings at a series of fixed temperatures in a manner which is very analogous to the heat-pulse method in calorimetry. The temperature interval between data points is 10% or less of the mean temperature at low temperatures, and is 5 K above 30 K. Thermal equilibrium is achieved in a matter of minutes at low temperatures, while up to 45 min are required at higher temperatures because of the increased heat capacities.

The length of the sample is the sum of the length of the upper capacitor reference rod  $L_c$  and the length of the capacitor gap  $L_g$ . The linear thermal-expansion coefficient [ $\alpha = L^{-1}(\partial L/\partial T)_P = \beta/3$  for cubic crystals such as the RGS] can be calculated from Eq. (2) and the capacitance change with temperature as

$$\alpha_{\text{RGS}} = \left( \frac{L_c + 2L_g}{L_c + L_g} \right) \alpha_{\text{Cu}} - \left( \frac{L_g}{L_g + L_c} \right) \frac{\Delta C}{C \Delta T}, \quad (4a)$$

where the factor 2 in the first term arises from the thermal expansion of the guarded capacitor plate, and  $\Delta C/\Delta T$  is negative. The linear thermal-expansion coefficient of copper varies from  $10^{-3}\alpha_{\text{RGS}}$  at low temperatures to a maximum of  $0.04\alpha_{\text{RGS}}$  at 105 K for xenon.<sup>18,24</sup> Since  $L_c = 2.9$  cm and  $L_g$  [from Eq. (2)] varies from 0.015 to 0.1 cm, Eq. (4a) can be simplified in practice to

$$\alpha_{\text{RGS}} = \alpha_{\text{Cu}} - \left( \frac{L_g}{L_g + L_c} \right) \frac{\Delta T}{C \Delta T}. \quad (4b)$$

The correction which should be applied to account for extraneous cell expansions (that is, the results of measurements with copper samples in the cell) is negligible for these RGS samples since it is typically 1 or 2% of  $\alpha_{\text{Cu}}$ .

$L_c$  is measured at room temperature with a micrometer to an accuracy of 0.1% or better. The diameter of the lower capacitor plate (approximate-

ly 1 cm) is measured with a traveling microscope to include one-half the 0.5-mm insulating gap between the plate and the guard ring. This measurement was checked by measuring the capacitance between the lower capacitor plate and a flat copper block which rested on sapphire spacers on the guard ring. The plate area then is obtained from the measured capacitance and the measured thickness of the spacers. Although this latter technique is limited by the accuracy of the measurement of the short spacers which were used and the lack of a perfectly coplanar guard ring and capacitor plate, and two determinations of the area agreed to within 0.2%. Both  $L_c$  and the area of the plate are corrected for temperature in the calculation of the thermal-expansion coefficient.

The raw unsmoothed and unscaled linear thermal-expansion coefficient  $\alpha$  data for all three RGS are given in Tables II–IV in the Appendix. Two sets of data were taken for all three solids, although only one set of samples was involved for each. Between these sets of data the samples were warmed up above their initial assembly temperature and remashed by not allowing them to expand as the temperature was increased. This resulted in a smaller low-temperature capacitor gap and hence a greater sensitivity for length changes. The smaller gap also tends to increase the sensitivity of the results to misalignment and other systematic errors. The argon and krypton samples were allowed to sublime during this process, so that there is a shift between the two sets of data, as is discussed below. The xenon was prevented from subliming during this process and the data reproduce well. Additional data which were taken on several argon samples are not given here since the samples contained what is believed to be an oxygen impurity.<sup>14</sup>

The existence of high-accuracy x-ray lattice-constant measurements as a function of temperature for argon<sup>8</sup> and krypton<sup>11</sup> allows an over-all check on the accuracy of the present data at higher temperatures. Such a comparison for two different sets of data is shown in Fig. 5 for the relative length change of krypton, where a smooth line has been drawn through the smoothed x-ray data points given by Losee *et al.*<sup>11</sup> Such comparisons always showed a difference of several percent, so a thorough investigation was made of the difference between the x-ray data and the capacitance cell data for both the argon and krypton thermal expansion and relative length change data above 20 K. This showed that the capacitance cell data always are larger than the x-ray data and, if the stated error of the x-ray data is taken into account, the ratio is temperature independent to within  $\pm 0.2\%$ . The ratio also is independent of the capacitor plate gap, which can increase by 40% between 25 and

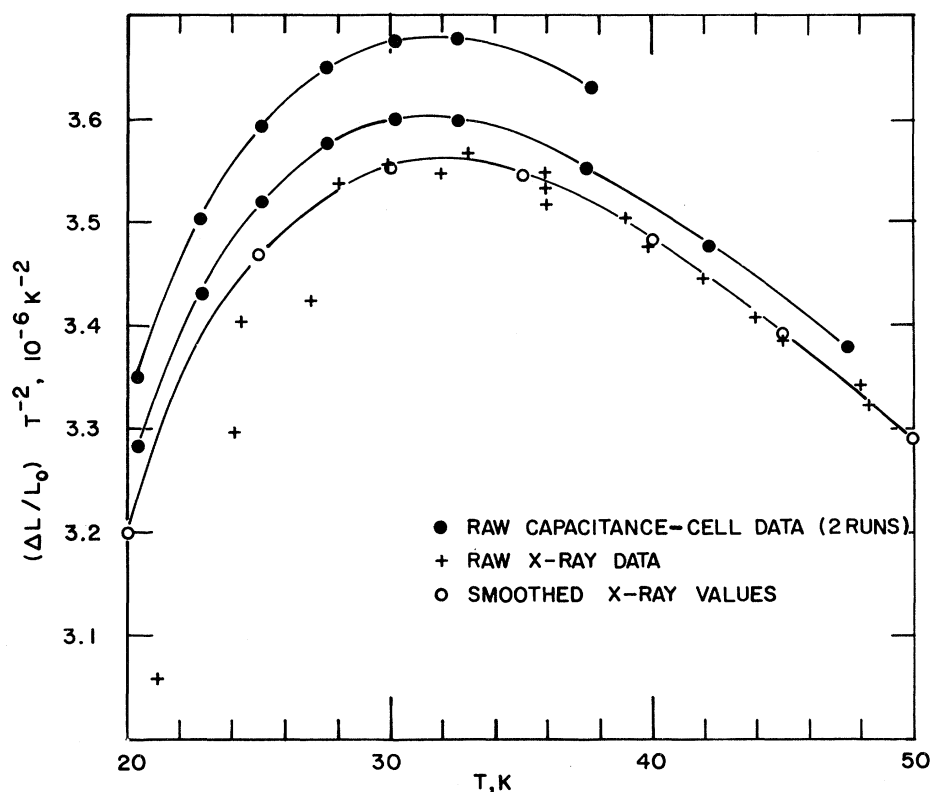


FIG. 5. Comparison for krypton of direct experimental capacitance-cell data with x-ray data (Ref. 11) to illustrate the systematic shift in the capacitance-cell data caused by sample bonding. The scale factors are 0.9 and 3.0% for the two sets of capacitance data.

35 K. If the samples are warmed to "high" temperatures between sets of data, e.g., 50–75 K for argon, but are not allowed to sublime, the two sets of data reproduce to within 0.2%. However, if the samples are warmed and the transfer tube connecting the capacitance cell to the bath stays cold so that the sample will sublime away to the cold spot fairly rapidly, the second set of data will be uniformly lower than the first set, but still higher than the x-ray data. In addition, except for krypton below 5 K, where instrumental difficulties were encountered, the different sets of capacitance cell data are consistent and reproducible to within the resolution of the apparatus at all temperatures.

These observations can be explained by the bonding of the samples to the copper cell parts. This constrains the ends of the samples to a constant diameter, so that the volume thermal expansion of a small length of the sample near the ends appears as an increased linear expansion. The magnitude of this effect is dependent on the ratio of the diameter of the end of the sample to the length of the sample. If the sample is warmed and allowed to sublime, the diameter is reduced while the length of the sample changes very little. The effect of the bonding, then, is reduced, as is the difference between the capacitance cell data and the x-ray data. The fact that no shift occurs in the data when the sample is prevented from subliming tends to con-

firm this explanation.

We therefore have scaled the argon and krypton data so that the high-temperature relative length-change data agree with the corresponding x-ray lattice-constant data above 25 K. Length change or integrated thermal-expansion data are used since the relative lattice-constant data are more accurate than the derived x-ray thermal-expansion data. The ratio to the x-ray data is temperature independent in the region where a meaningful comparison can be made, and we assume that it remains temperature independent at low temperatures. Keeler and Batchelder<sup>25</sup> observed unexpected behavior for the elastic constants of solid argon below 15 K, which they ascribe to a cessation of strain relief between the transducer and sample below that temperature. However, the thermal expansion and attendant strain are rapidly decreasing at these temperatures and one would not expect to see a radical change in the strains at low temperatures. Furthermore, except for the low-temperature krypton data previously mentioned, all of the data on all of the samples are smooth and reproducible to within the instrumental resolution in spite of a wide variety of assembly temperatures, cooling and warming rates, and annealing times. If some anomaly occurs in the thermoelastic properties of the solids, one would not expect the data to be smooth and independent of thermal history.

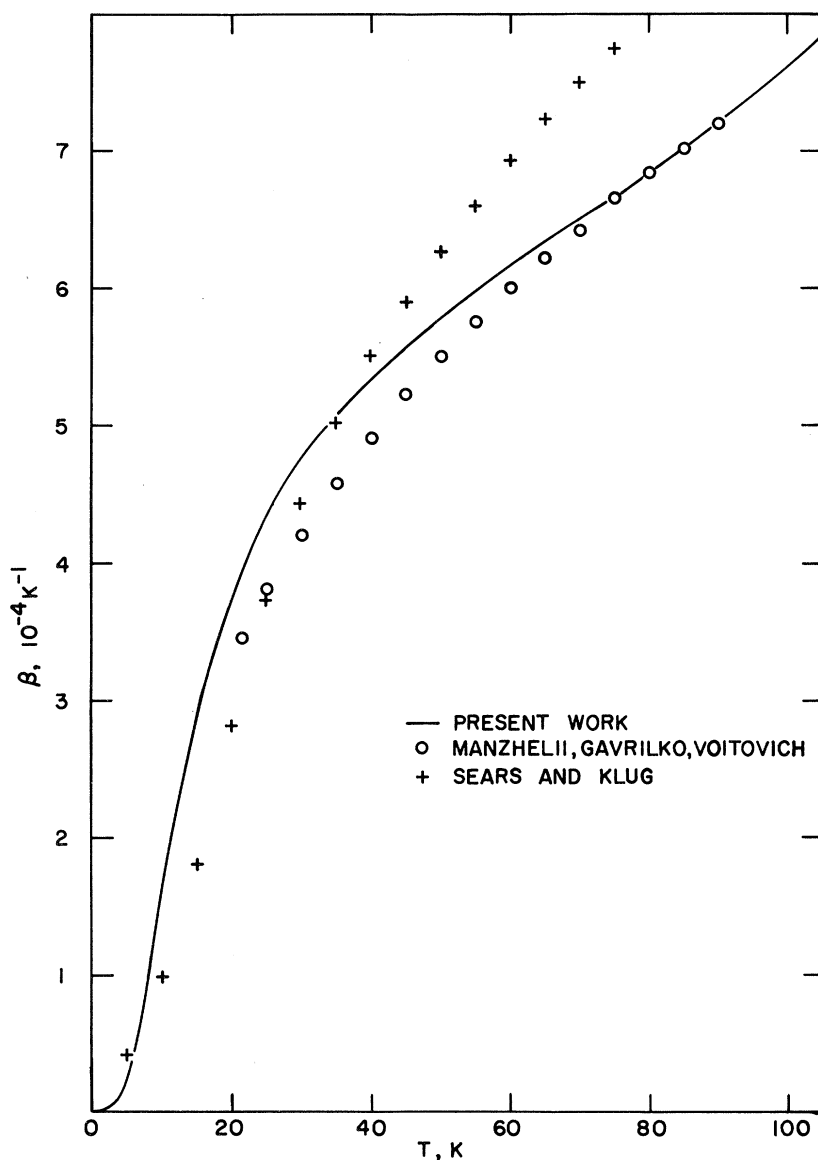


FIG. 6. Present data for xenon compared with quartz dilatometer (Ref. 27) (O), and polycrystalline x-ray (Ref. 26) data (+). The present data may be systematically high by several percent over the entire temperature range.

High-precision x-ray measurements do not yet exist for xenon, so a comparison of the type made for argon and krypton cannot be made. Figure 6 shows the present data compared with polycrystalline x-ray data<sup>26</sup> and the quartz dilatometer measurements of Manzhelii, Gavrilko, and Voitovich.<sup>27</sup> Unfortunately, a steady decrease in the length of our samples at constant temperature around 75 K indicated that they were beginning to sublime. Sublimation was inhibited by the addition of more exchange gas at different temperatures above 75 K, so that the data between 75 and 105 K are somewhat unreliable. It is not clear if the agreement with the data of Manzhelii *et al.*<sup>27</sup> above 75 K is significant, or whether indeed our  $\alpha$ 's are too large in this region. The sample bonding and sublimation

effects tend to introduce uncertainties of opposite sign in the measured expansion coefficients, and the xenon results could be affected by both of these.

#### DISCUSSION

Smoothed values for the volume thermal-expansion coefficient ( $\beta = 3\alpha$ ) and the integrated linear thermal expansions  $\Delta L/L_0$  are given for each of these solids in Table I. The argon results are those of set I, and the  $\alpha$ 's have been smoothed and scaled by 3.5% to agree with the high-temperature x-ray data. The krypton results are those of set I also, similarly smoothed and scaled by 3.0%, except for the 40- and 45-K points, which are from set II and which have been scaled by 0.9%. Although set II of the krypton data is more complete



TABLE I. Smoothed volume-thermal-expansion coefficients and relative length changes for argon, krypton, and xenon.

T (K)	Argon		Krypton		Xenon	
	$\beta$ (K <sup>-1</sup> )	$\Delta L/L_0$	$\beta$ (K <sup>-1</sup> )	$\Delta L/L_0$	$\beta$ (K <sup>-1</sup> )	$\Delta L/L_0$
1	$1.03 \times 10^{-7}$	$8.52 \times 10^{-9}$	$1.50 \times 10^{-7}$	$1.25 \times 10^{-8}$	$1.53 \times 10^{-7}$	$1.265 \times 10^{-8}$
1.5	3.50	$4.343 \times 10^{-8}$	5.17	6.39	5.29	6.51
2	8.40	$1.385 \times 10^{-7}$	$1.250 \times 10^{-6}$	$2.05 \times 10^{-7}$	$1.289 \times 10^{-6}$	$2.107 \times 10^{-7}$
2.5	$1.671 \times 10^{-6}$	3.423	2.510	5.10	2.644	5.30
3	2.948	7.21	4.485	$1.082 \times 10^{-6}$	4.800	$1.137 \times 10^{-6}$
3.5	4.796	$1.356 \times 10^{-6}$	7.39	2.058	8.06	2.191
4	7.36	2.358	$1.150 \times 10^{-5}$	3.614	$1.278 \times 10^{-5}$	3.927
4.5	$1.080 \times 10^{-5}$	3.859	1.712	5.98	1.877	6.56
5	1.531	6.02	2.438	9.44	2.640	$1.032 \times 10^{-5}$
5.5	2.111	9.03	3.328	$1.424 \times 10^{-5}$	3.555	1.548
6	2.845	$1.316 \times 10^{-5}$	4.383	2.067	4.614	2.229
6.5	3.713	1.862	5.60	2.899	5.80	3.097
7	4.751	2.568	6.96	3.946	7.09	4.171
7.5	5.94	3.458	8.46	5.23	8.44	5.47
8	7.27	4.559	$1.005 \times 10^{-4}$	6.77	9.86	6.99
8.5	8.74	5.89	1.172	8.59	$1.134 \times 10^{-4}$	8.76
9	$1.034 \times 10^{-4}$	7.49	1.349	$1.069 \times 10^{-4}$	1.281	$1.077 \times 10^{-4}$
9.5	1.206	9.35	1.527	1.309	1.428	1.303
10	1.386	$1.151 \times 10^{-4}$	1.709	1.578	1.577	1.553
10.5	1.573	1.397	1.896	1.900	1.724	1.828
11	1.768	1.676	2.082	2.086	1.866	2.127
12	2.74	2.332	2.444	2.965	2.139	2.795
13	2.595	3.127	2.796	3.838	2.395	3.550
14	3.024	4.065	3.135	4.825	2.636	4.387
15	3.455	5.14	3.460	5.92	2.860	5.30
16	3.886	6.37	3.767	7.12	3.069	6.29
18	4.748	9.25	4.323	9.83	3.438	8.46
20	5.51	$1.266 \times 10^{-3}$	4.819	$1.288 \times 10^{-3}$	3.738	$1.085 \times 10^{-3}$
25	7.20	2.331	5.79	2.175	4.341	1.761
30	8.57	3.646	6.53	3.205	4.749	2.520
35	9.75	5.17	7.08	4.344	5.08	3.341
40	...	...	7.56	5.57	5.34	4.213
45	...	...	7.98	6.87	5.57	5.13
50	...	...	...	...	5.77	6.08
55	...	...	...	...	5.96	7.06
60	...	...	...	...	6.15	8.08
65	...	...	...	...	6.33	9.12
70	...	...	...	...	6.50	$1.020 \times 10^{-2}$
75	...	...	...	...	6.66	1.131
80	...	...	...	...	6.83	1.245
85	...	...	...	...	7.01	1.361
90	...	...	...	...	7.20	1.481
95	...	...	...	...	7.40	1.605
100	...	...	...	...	7.61	1.732
105	...	...	...	...	7.84	1.863

and of higher resolution, the low-temperature data for this set are less reliable because of experimental difficulties. The xenon results are smoothed but unscaled.

The low-temperature data for all three samples are presented in Fig. 7 in the form of a reduced  $\beta/T^3$ -vs- $T^2$  plot. The data are as taken, except that the argon and krypton data points have been scaled as above. The appropriate coefficients for the  $aT^3 + bT^5$  relations are given in the figure.

The present results for krypton (Table I) can be compared directly with the smoothed optical interferometer results of Korpium and Coufal,<sup>13</sup> which are identical with the x-ray results<sup>11</sup> from 10 to 80 K. These authors also report a smoothed value of  $\beta$  for 5 K ( $3.8 \pm 0.02 \times 10^{-5}$  K<sup>-1</sup>), which is identical again with a smooth x-ray value which appears to have been obtained by interpolation between the 4- and 6-K values given by Losee *et al.*<sup>11</sup> Our smoothed results, which were normalized to the

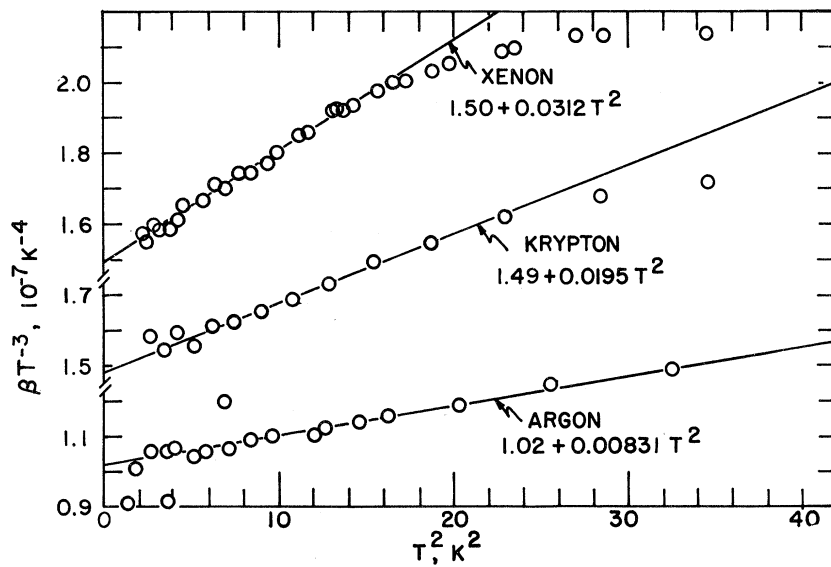


FIG. 7. Unsmoothed low-temperature data for all three samples. The xenon data are from both sets I and II and are unscaled. The krypton data are from set I, as scaled by 3.0%, and the argon data are from set I, as scaled by 3.5%.

x-ray results between 25 and 45 K, must agree with the smoothed interferometric results in this region. From 10 to 25 K, these smoothed results (and the smoothed results of Losee *et al.*<sup>11</sup>) lie  $(2.5 \pm 1)\%$  lower than ours. This is a factor of 2 greater than the error limits which are quoted for the x-ray work ( $\pm 0.5 \times 10^{-5} \text{ K}^{-1}$ ) and is a factor of 3 or 4 greater than that which can be estimated from the optical interferometer resolution (300 Å) and the 5.3-cm-long samples.<sup>12</sup> We feel that the differences from 10 to 20 K perhaps are reasonable and reflect systematic errors in at least one of the experiments. The excellent agreement between the smoothed optical and x-ray volume thermal-

expansion results between 10 and 80 K (to  $0.1 \times 10^{-5} \text{ K}^{-1}$ ) must be regarded as fortuitous since it is at least a factor of 5 better than the combined estimated uncertainties in the two sets of data.

The present data and the smoothed optical interferometer results disagree violently at 5 K, where our value of  $2.44 (\pm 0.02) \times 10^{-5} \text{ K}^{-1}$  is to be compared with the interferometric value of  $3.8 (\pm 0.02) \times 10^{-5} \text{ K}^{-1}$ . We feel that our results are to be preferred, in part because the capacitance method has roughly 100 times greater resolution than the optical interferometer at this temperature, and in part because of the reproducibility of our data when different capacitor gaps are used. Indeed, the

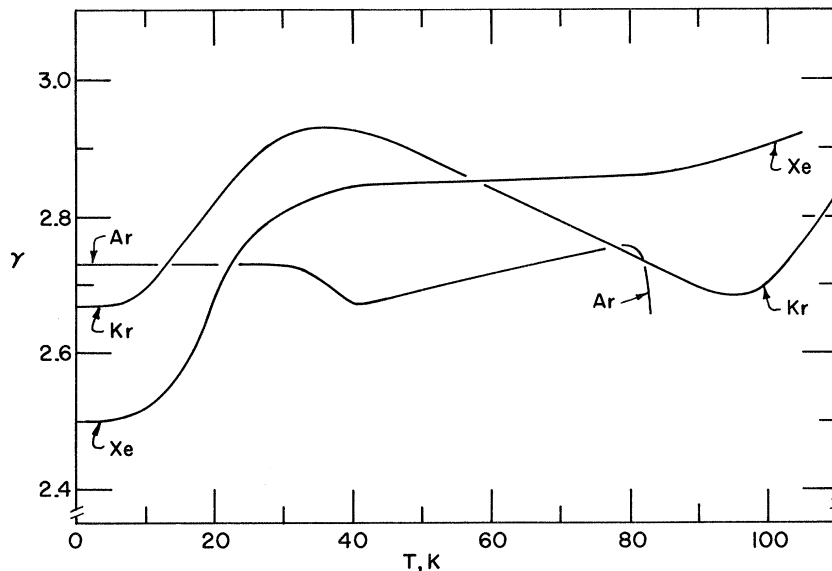


FIG. 8. The temperature dependence of the Grüneisen parameter  $\gamma$  for all three solids. X-ray values have been included at higher temperatures for completeness.

existence of this internal check for the present data indicates that these should be accurate in a relative sense to better than 1% at all temperatures between 5 and 40 K. In addition, the optical interferometer value for  $\beta$  results in an anomalously high value of the Grüneisen parameter at 5 K (4.1), while our data (see below) give a 5-K value (2.60) which is just slightly smaller than the value at 10 K (2.69). This latter would appear to be the "normal" behavior. The reason for the large 5-K discrepancy in  $\beta$  is not clear, although it may have arisen due to the rapid decrease in the relative sensitivity of the optical interferometer at temperatures approaching absolute zero.

The Grüneisen parameters which are plotted in Fig. 8 are calculated from the relation

$$\gamma = \beta B_T V / C_V = \beta B_S V / C_P. \quad (5)$$

We have used the ultrasonic value for  $B_S$  for argon, as given by Keeler and Batchelder<sup>25</sup> for temperatures above 30 K. There is reason to mistrust these data below 30 K<sup>4</sup> as well as the x-ray value for  $B_T$  at 4.2 K given by Urvas *et al.*,<sup>4,9</sup> so we have assumed a  $T=0$  theoretical value of  $B_T$  (29.2 kbar) for argon,<sup>4</sup> and have extrapolated the ultrasonic data to this value for temperatures below 30 K. The resulting curve agrees to better than 5% with recent  $B_T$  data obtained in this laboratory.<sup>28</sup> The other  $B_T$  data are from Urvas *et al.*<sup>9</sup> for krypton (which agree with the interferometer results<sup>12,13</sup>) and from Anderson and Swenson for xenon.<sup>28</sup> The Anderson and Swenson data are obtained using the piston-displacement technique in a manner similar to that used by Packard and Swenson<sup>29</sup> in earlier work on xenon, although with improved accuracy. These experiments give results for krypton which agree very well with the other existing zero-pressure data for this solid<sup>9,12,13</sup> and also agree to better than 5% with the earlier xenon data.<sup>29</sup>

Since the heat-capacity data are for the most part available directly as  $C_P$  at zero pressure, we have converted  $B_T$  to  $B_S$  using the relation

$$B_S^{-1} = B_T^{-1} - TV\beta^2/C_P.$$

The molar volumes  $V$  in all cases originate from a combination of the x-ray lattice-parameter data and the thermal-expansion data. There is some disagreement between the two sets of  $C_P$  data which are available for both argon<sup>30,31</sup> and krypton.<sup>31,32</sup> Hence, we have used both of these in calculating the  $\gamma$ 's, and have drawn a smooth curve through the results by making the assumption that  $\gamma$  must be a smooth value of the temperature. In particular, the  $C_P$  results of Finegold and Phillips<sup>31</sup> appear to be a bit (2%) high near 4.5 K and possibly near 12.5 K. On the other hand, the data of Flubacher *et al.*<sup>30</sup> for argon and Beaumont *et al.*<sup>32</sup> for krypton, which were obtained using the same

apparatus, appear to be slightly high near 8 K. The problems apparently do not lie in the thermal-expansion measurements nor in the bulk-modulus values (which may be uncertain systematically to 5% or so) since the  $\gamma$ -vs- $T$  curves are smooth for one set of data and not for the other near each of these temperatures. High-temperature  $C_V$  data also exist for argon.<sup>33</sup> The heat-capacity data for xenon are from the work of Serin and his co-workers.<sup>34,35</sup>

The curves in Fig. 8 also include high-temperature results which are based on the x-ray data of Simmons and his co-workers.<sup>8,11</sup> The differences from the values given in the earlier work for argon<sup>8</sup> arise because of the use of the more recent bulk-modulus and  $C_P$  data.

#### Sources of Error

The temperature measurements are sufficiently precise that the error in  $\alpha$  due to  $\Delta T$  is less than 0.3% below 2 K and is significantly less above 2 K. The maximum uncertainty of 0.2% in the temperature around 4 K contributes an error of about 0.6% in the thermal expansion. Any error due to inaccuracy in an individual capacitance measurement is less than 0.02%. Below 3 K, however, the resolution of the capacitance measurement becomes a limitation and contributes up to a 2% error. Above 4 K the resolution of the data is limited primarily by temperature control and generally is of the order of 0.2%. If the temperature is not changed monotonically, a small hysteresis is evident in the length change. However, if the temperature change is monotonic, the  $\alpha$  data reproduce to within 0.2% above 4 K, and data taken with decreasing temperature agree with those taken with increasing temperature to within 0.3%. Because of convenience, most data were taken with the temperature increasing. Systematic errors due to inaccuracies in the measurement of the capacitor cell parts should not exceed  $\pm 0.2\%$ . The total error in the thermal-expansion measurements, excluding the systematic shift due to sample bonding, should be less than  $\pm 0.7\%$  above 5 K, and less than  $\pm 1.5\%$  below 5 K. The use of a  $\beta/T^3$ -vs- $T^2$  plot at low temperatures aids significantly in the determination of the form of this low-temperature  $\beta$ -vs- $T$  relation.

The error introduced by the sample bonding is more difficult to assess. As discussed previously, we are confident that it is temperature independent. If this is so, the scaling to fit the x-ray data introduces only a small error, so that the scaled argon and krypton thermal-expansion values are probably accurate to about  $\pm 1\%$  above 5 K and  $\pm 2\%$  below 5 K. The xenon data agree quite well with these of Manzhelii *et al.*<sup>27</sup> at higher temperatures, but the stated accuracy of that work is 5%, so the

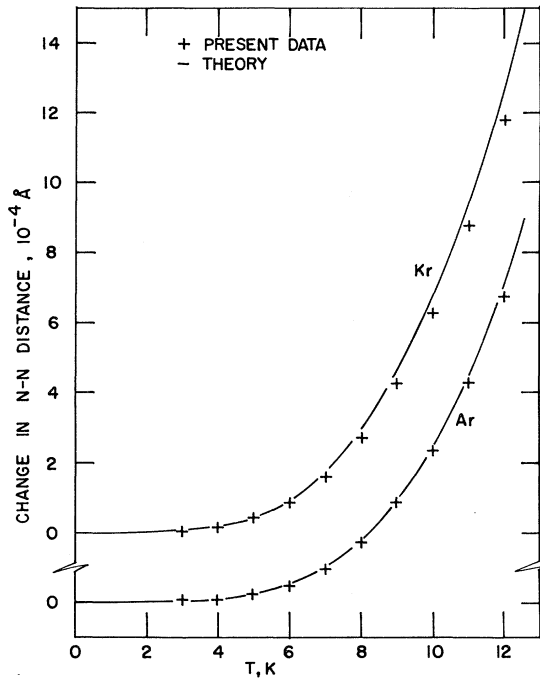


FIG. 9. Theoretical results for the change in nearest-neighbor (NN) distance (Refs. 5, 6, and 36) compared with the present results. See the text for details.

agreement is not necessarily significant. However, judging from the experience with argon and krypton, it is unlikely that the error due to bonding in the

TABLE II. Experimental unscaled linear-thermal-expansion data for solid argon.

$T$ (K)	$\alpha$ (K <sup>-1</sup> )	$T$ (K)	$\alpha$ (K <sup>-1</sup> )
Set I			
1.323	$8.04 \times 10^{-8}$	16.957	1.478
1.595	$1.47 \times 10^{-7}$	19.447	$1.823 \times 10^{-4}$
1.917	2.56	26.989	2.679
1.123	$4.43 \times 10^{-8}$	28.946	2.863
1.978	$2.83 \times 10^{-7}$	30.945	3.037
2.257	4.12	32.982	3.207
2.669	6.95	34.962	3.361
Set II			
3.098	$1.124 \times 10^{-6}$	11.399	$6.61 \times 10^{-5}$
3.548	1.720	13.862	$1.015 \times 10^{-4}$
4.026	2.587	16.611	1.414
4.506	3.726	19.882	1.854
5.051	5.50	22.950	2.225
5.696	8.23	26.243	2.565
6.420	$1.229 \times 10^{-5}$	29.530	2.864
7.197	1.796	32.536	3.113
8.045	2.551	35.518	3.338
9.101	3.683	38.454	3.544
10.350	5.23	26.970	2.644
11.751	7.15	28.948	2.825
13.284	9.26	30.943	2.995
14.950	$1.185 \times 10^{-4}$		

TABLE III. Experimental unscaled linear-thermal-expansion data for solid krypton.

$T$ (K)	$\alpha$ (K <sup>-1</sup> )	$T$ (K)	$\alpha$ (K <sup>-1</sup> )
Set I			
1.635	$2.381 \times 10^{-7}$	11.163	7.35
1.846	3.34	12.101	8.51
2.041	4.66	13.323	9.99
2.252	6.11	14.658	$1.149 \times 10^{-4}$
2.484	8.47	16.119	1.307
2.730	$1.136 \times 10^{-6}$	17.698	1.457
2.999	1.539	19.441	1.609
3.287	2.064	21.572	1.770
3.587	2.753	23.909	1.922
3.930	3.747	26.300	2.061
4.328	5.14	28.854	2.188
4.786	7.25	31.340	2.298
5.322	$1.026 \times 10^{-5}$	35.091	2.436
Set II			
5.881	1.413	1.484	$1.69 \times 10^{-7}$
6.471	1.897	1.645	2.27
7.120	2.509	1.820	3.11
7.830	3.260	2.009	4.22
8.782	4.372	2.219	5.71
9.611	5.38	2.449	7.84
10.332	6.29	6.477	1.893
1.565	1.93	16.820	$1.346 \times 10^{-4}$
1.763	2.82	18.071	1.462
2.025	4.38	19.457	1.577
2.273	6.14	21.591	1.733
2.491	8.30	23.931	1.883
3.009	$1.516 \times 10^{-6}$	26.324	2.017
3.309	2.074	28.880	2.142
3.606	2.753	31.336	2.243
3.936	3.705	34.985	2.371
4.338	5.107	39.851	2.534
4.763	7.03	44.853	2.676
5.300	$1.004 \times 10^{-5}$		
5.891	1.403		

xenon data is greater than 3%.

The errors in the Grüneisen parameters are rather difficult to assess since they involve the individual errors in the thermal-expansion, heat-capacity, and bulk-modulus measurements, not all of which are given in the literature. The thermal-expansion and heat-capacity values should be most accurate at higher temperatures. The bulk moduli, on the other hand, are most accurate at low temperatures, but in any event are relatively poorly known. It appears that the  $\gamma$ 's for argon and krypton are probably accurate to within  $\pm 3\%$  while the argon and xenon values are probably good to  $\pm 5\%$ .

Several of the argon samples measured in the initial experiments showed a low-temperature anomaly which was ascribed to oxygen impurities entering through leaks in the gas-handling system during sample growth.<sup>14</sup> A leak-tight glass gas-handling system was used for all subsequent samples and the samples were grown in the capacitance

TABLE IV. Experimental unscaled linear-thermal-expansion data for solid xenon.

$T$ (K)	$\alpha$ (K <sup>-1</sup> )	$T$ (K)	$\alpha$ (K <sup>-1</sup> )
Set I			
2.520	$9.11 \times 10^{-7}$	18.221	1.158
2.769	$1.233 \times 10^{-6}$	20.035	1.250
3.044	1.665	22.058	$1.337 \times 10^{-4}$
3.352	2.322	24.268	1.425
3.695	3.236	27.716	1.493
4.063	4.467	29.227	1.566
4.437	5.98	31.475	1.619
4.846	7.96	34.969	1.691
5.335	$1.079 \times 10^{-5}$	39.956	1.778
5.868	1.443	44.958	1.854
6.498	1.933	49.965	1.921
7.200	2.542	54.973	1.986
7.850	3.139	59.987	2.049
8.644	3.923	64.979	2.111
9.593	4.850	70.271	2.171
10.528	5.77	74.984	2.215
11.554	6.73	79.318	2.250
12.709	7.74	84.328	2.339
13.823	8.65	89.997	2.387
15.043	9.56	95.043	2.426
16.563	$1.059 \times 10^{-4}$	100.052	2.542
		104.935	2.611
Set II			
1.539	$1.88 \times 10^{-7}$	3.145	1.869
1.763	2.91	3.426	2.497
2.024	4.45	3.770	3.451
1.487	1.89	3.008	1.644
1.705	2.64	3.311	2.255
1.935	3.84	3.615	3.019
2.150	5.49	3.943	4.033
2.375	7.44	4.341	5.55
2.623	$1.025 \times 10^{-6}$	4.769	7.56
2.886	1.398	5.298	$1.057 \times 10^{-5}$
		5.880	1.450

cell so that they did not have to be transferred from one Dewar to another. Only one of these later samples showed any sign of an anomaly and that was an argon sample believed contaminated when air entered the sample chamber when difficulties were encountered in the assembly procedure. The data in Fig. 7 show no trace of a low-temperature anomaly in any of the three samples, indicating that no significant amount of air was present in any of the samples. The gases used were all of 99.999% initial purity and care was taken to purge the mold and all connecting lines of contaminant gases.

#### CONCLUSIONS

The primary temperature dependence of the thermal-expansion coefficient is almost identical with that of the specific heat for those solids.

Hence, the thermal-expansion-related quantity which is of greatest interest is the Grüneisen parameter  $\gamma$  [Eq. (5)].

In essence,  $\gamma$  is the only solid-state parameter that can be evaluated at constant pressure which yields information about the third derivatives of the potential function with respect to interatomic spacing. The suppressed zero in Fig. 8 gives the misleading impression that the  $\gamma$ 's for these solids are strongly temperature dependent, while in fact they are not, since the maximum variation for any individual solid is just over 10%. Indeed the maximum difference between the  $\gamma$ 's at a given temperature is only 10%, which is to be compared with the inherent uncertainties of from 3 to 5% in the bulk moduli (and hence in the  $\gamma$ 's). The  $\gamma$ -vs- $T$  relation for krypton is perhaps the most reliable since several independent determinations of the bulk modulus exist for this solid. We also have considerable confidence in the bulk moduli and their temperature dependence for xenon, with estimated uncertainties ranging from 3% at 4 K to 5% at 100 K.<sup>28</sup> The argon curve appears to be quite different from the others, but for various reasons the bulk-modulus data are more poorly determined experimentally for this solid than for the other two, and the shape of the  $\gamma$ -vs- $T$  curve depends very strongly on the  $B_T$ -vs- $T$  relation which is used in its calculation. This occurs since, contrary to the behavior of most other solids, the bulk moduli of the inert gas solids are very strongly temperature dependent, with triple-point values of  $B_T$  which are roughly one-third of their  $T=0$  values.<sup>9,25,28,29</sup>

Klein *et al.*<sup>3</sup> have compared the results of high-temperature improved self-consistent phonon calculations for these solids with lower-temperature perturbation-theory calculations and have demonstrated that the  $\gamma$ 's are independent of the computation method in an overlap region. These calculations appear to agree with the present data to within 5% at all temperatures where the calculations are valid (above 7 K). The calculated  $\gamma$ 's increase from argon to krypton to xenon at low temperature, while we appear to observe the opposite effect, but the differences are small in absolute magnitude and most likely are not significant.

The results of these calculations are open to some question, however, since they are based on a two-body potential of the Lennard-Jones type, and recent theoretical work on the thermodynamic properties of solid argon<sup>4,5,36</sup> and solid krypton<sup>6</sup> has shown that this assumption is unrealistic. In particular, these new calculations have used a modified form of the Barker-Pompe potential for two-body interactions and have included the Axilrod-Teller triple-dipole interaction in a perturbation-theory calculation. When these calculations are refined to include self-consistent phonon ef-

fects, one would hope to have a better basis for comparing the present data with theory, either directly through the thermal-expansion coefficients or through the  $\gamma$ 's. Our data for the temperature variation of the nearest-neighbor distance are compared with these calculations<sup>5,6,37</sup> in Fig. 9.

The above discussion of the present data and their relationship to other data such as those for the specific heat and the bulk modulus suggest the existence of gaps in our experimental knowledge of the thermodynamic properties of these solids. The presentation of the results in terms of Grüneisen parameters is limited primarily by the uncertainties in the bulk-modulus data, although more precise low-temperature heat-capacity data would be useful especially for xenon. The small uncertainties in the present values of the thermal-expansion coefficients are the least significant factor in the discussion of these calculations.

#### ACKNOWLEDGMENTS

The authors are indebted to M. S. Anderson,

J. C. Holste, and Dr. R. Q. Fugate for their assistance at critical times during the carrying out of these measurements. We also have profited from conversations with Dr. J. A. Barker. We gratefully acknowledge the receipt before publication of results from Dr. Barker and Dr. P. Korpium and Dr. J. Coufal.

#### APPENDIX

In Tables II–IV are a tabulation of the experimental linear-thermal-expansion data for solid argon, krypton, and xenon. All data for a given solid are for a single set of samples with, however, the capacitance-cell gap made smaller for the second set in each case by heating the cell to a temperature greater than the initial assembly temperature. These data have not been scaled or smoothed in any manner. The text gives the details of the manner in which these data were scaled to obtain the smoothed values given in Table I.

\*Contribution No. 3049. This work was performed in the Ames Laboratory of the U. S. Atomic Energy Commission.

†Present address: Pressure Section, Heat Division, National Bureau of Standards, Washington, D. C.

<sup>1</sup>G. K. Horton, *Am. J. Phys.* **36**, 94 (1968).

<sup>2</sup>N. R. Werthamer, *Am. J. Phys.* **37**, 763 (1969).

<sup>3</sup>M. L. Klein, V. V. Goldman, and G. K. Horton, *J. Phys. Chem. Solids* **31**, 2441 (1970).

<sup>4</sup>M. V. Bobetic and J. A. Barker, *Phys. Rev. B* **2**, 4196 (1970).

<sup>5</sup>J. A. Barker, M. L. Klein, and M. V. Bobetic, *Phys. Rev. B* **2**, 4176 (1970).

<sup>6</sup>J. A. Barker, M. V. Bobetic, and M. L. Klein, *Phys. Letters* **34A**, 415 (1971).

<sup>7</sup>G. E. Jelinek, *Phys. Rev. B* **3**, 2716 (1971).

<sup>8</sup>O. G. Peterson, D. N. Batchelder, and R. O. Simmons, *Phys. Rev.* **150**, 703 (1966).

<sup>9</sup>A. O. Urvas, D. L. Losee, and R. O. Simmons, *J. Phys. Chem. Solids* **28**, 2269 (1967).

<sup>10</sup>D. N. Batchelder, D. L. Losee, and R. O. Simmons, *Phys. Rev.* **162**, 767 (1967).

<sup>11</sup>D. L. Losee and R. O. Simmons, *Phys. Rev.* **172**, 944 (1968).

<sup>12</sup>R. Veith, H. J. Coufal, P. Korpium, and E. Lüscher, *Z. Angew. Phys.* **29**, 153 (1970); *J. Appl. Phys.* **41**, 5082 (1970).

<sup>13</sup>P. Korpium and H. J. Coufal, *Phys. Status Solidi* **A6**, 187 (1971).

<sup>14</sup>C. R. Tilford and C. A. Swenson, *Phys. Rev. Letters* **22**, 1296 (1969).

<sup>15</sup>D. C. Heberlein and E. D. Adams, *J. Low Temp. Phys.* **3**, 115 (1970).

<sup>16</sup>D. C. Heberlein, E. D. Adams, and T. A. Scott, *J. Low Temp. Phys.* **2**, 449 (1970).

<sup>17</sup>G. K. White, *Cryogenics* **1**, 151 (1961).

<sup>18</sup>R. H. Carr, R. D. McCammon, and G. K. White, *Proc. Roy. Soc. (London)* **280**, 72 (1964).

<sup>19</sup>A. M. Thompson, *IRE Trans. Instr.* **7**, 245 (1958).

<sup>20</sup>Laird C. Towle, *Appl. Phys. Letters* **10**, 317 (1967).

<sup>21</sup>J. S. Rogers, R. J. Tainsh, M. S. Anderson, and C. A. Swenson, *Metrologia* **4**, 47 (1968).

<sup>22</sup>T. C. Cetas, C. R. Tilford, and C. A. Swenson, *Phys. Rev.* **174**, 835 (1968).

<sup>23</sup>T. C. Cetas and C. A. Swenson, *Phys. Rev. Letters* **25**, 338 (1970); also to be published in *Metrologia*; also in the *Proceedings of the Fifth Symposium on Temperature* (unpublished).

<sup>24</sup>T. Rubin, H. W. Altman, and H. L. Johnston, *J. Am. Chem. Soc.* **76**, 5289 (1954).

<sup>25</sup>G. J. Keeler and D. N. Batchelder, *Proc. Phys. Soc. (London)* **3**, 510 (1970).

<sup>26</sup>D. R. Sears and H. P. Klug, *J. Chem. Phys.* **37**, 3002 (1962).

<sup>27</sup>V. G. Manzhelii, V. G. Gavrilko, and E. I. Voitovich, *Fiz. Tverd. Tela* **9**, 1483 (1967) [*Sov. Phys. Solid Chem.* **9**, 1157 (1967)].

<sup>28</sup>M. S. Anderson and C. A. Swenson (unpublished).

<sup>29</sup>J. R. Packard and C. A. Swenson, *J. Phys. Chem. Solids* **24**, 1405 (1963).

<sup>30</sup>P. Flubacher, A. J. Leadbetter, and J. A. Morrison, *Proc. Phys. Soc. (London)* **78**, 1449 (1961).

<sup>31</sup>L. Finegold and N. E. Phillips, *Phys. Rev.* **172**, 944 (1968).

<sup>32</sup>R. H. Beaumont, H. Chihara, and J. A. Morrison, *Proc. Phys. Soc. (London)* **78**, 1462 (1961).

<sup>33</sup>F. Haenssler, K. Gamper, and B. Serin, *J. Low Temp. Phys.* **3**, 23 (1970).

<sup>34</sup>H. Fenichel and B. Serin, *Phys. Rev.* **142**, 490 (1966).

<sup>35</sup>J. U. Trefny and B. Serin, *J. Low Temp. Phys.* **1**, 231 (1969).

<sup>36</sup>M. L. Klein, J. A. Barker, and T. R. Koehler, *Phys. Rev. B* **4**, 1933 (1971).

<sup>37</sup>J. A. Barker (private communication).